A Review on Metasurface and Metamaterials for Antenna Design

M. Vinodkumar
Department of ECE, CCET Chandigarh, India

Dinesh Sharma
Sri Vasavi engineering college, India
Corresponding author: M. Vinodkumar, Email: mvkumar465@gmail.com

The primary goal of this review paper is to present the fundamentals of left-handed materials and the silent features and drawbacks of Metamaterial, and the recent development of Metasurface antennas. Metamaterials are made up of periodic sub-wavelength structures resonantly related to the electric and magnetic fields of incident electromagnetic waves and possess unique features that do not present in naturally occurring materials. Metamaterials are challenging to fabricate due to their 3D geometry complexity, while Metasurface are easy to fabricate due to their planar structure. The specific properties and uses of Metamaterial and Metasurface are discussed in this work, as well as cloaking systems, phase correction methods, and perfect lenses.

Keywords: Metamaterial, Metasurface, Left-handed materials, Cloaking devices.

2021. In Rahul Srivastava & Aditya Kumar Singh Pundir (eds.), *New Frontiers in Communication and Intelligent Systems*, 185–205. Computing & Intelligent Systems, SCRS, India. https://doi.org/10.52458/978-81-95502-00-4-22

1 Introduction

Microstrip patch antenna has played an essential role in booming technology over the last few decades due to its small scale and low profile antenna [1]. A standard microstrip patch antenna consists of a three-dimensional substrate with the radiating portion on one side and the ground on the other [2]. Standard MPA has several drawbacks, including poor radiation efficiency, narrow Bandwidth, and low Gain. Several techniques like Defect ground structure can overcome those defects, Electronic band gap structure, Reconfigurable antenna, Fractal antennas, etc.[3-6], but in all the earlier stated techniques, radiation efficiency cannot achieve maximum along with the wide Bandwidth, high Gain and Size reduction [7-8].

Over the last few years, Left-handed materials have played a vital role due to several advantages like good Radiation efficiency, High Bandwidth, Good polarization conversion ratio, etc., due to their unique properties, which can't exist in the natural material [9].

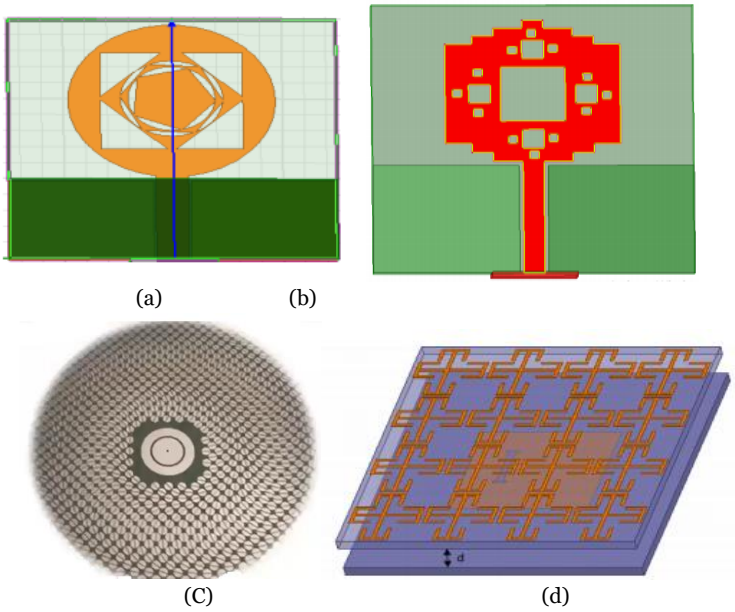

Fig. 1. a, b shows the microstrip patch antenna with Right-hand material [3,7]
c, d shows the patch antenna with the Left-handed material [64,35]

2 Materials and its Types

Generally, the material is a mixture of the substances which constitute the object. Several materials are available for implementing the microstrip antennas with positive permittivity and permeability, such as FR4, Rogers, Bakelite, etc. These materials can be termed as Right-handed material (RHM).

There are some materials with negative permittivity and permeability that are not available naturally. These materials can be called Left-handed materials. They are mainly three types. 1. Epsilon negative material (ENG). 2. Mu negative material (MNG), 3. Double negative material (DNG).

(a) Left-handed materials

Metamaterial is a word count from the Seminar paper [9] by Pendry. The optical lens is the primary tool from the past 19th century, and it can be used either by polishing the lens or changing the

dielectric material. According to Pendry, the ideal lens can only be made possible by artificial materials, which cannot be made from natural materials and have unique properties. Negative permittivity and permeability are desirable [9]. Later, Vassalage and Smith, along with Pendry, created these artificial mediums. Metamaterial was suggested as a title for these unique properties at the international conference in 2004. Metamaterial can be derived from the Greek word Meta which means beyond, and Material can be from the Latin word Meta. Metamaterial is a 3-dimensional material with subwavelength inclusions and effective fundamental parameters not occurring in the natural material [10]. A good radiation efficiency, Reduction in the size, wider Bandwidth had been achieved by using the Metamaterials. The major limitation in this is that a large-scale production cannot be possible, and losses would also occur during the large production with these three-dimensional metamaterials [11].

Metasurface is a 2-dimensional material with unique properties like relative permittivity, and relative permeability should be negative as Metamaterial [12]. Metasurface is a simple planar structure with a two-dimensional material, while Metamaterial is a three-dimensional material. Due to the simple design of the MTS, fabrication is also easy and cost-effective. Metasurface has several applications as the Metamaterial like an invisible cloak, perfect lens, phase compensators, high radiators [13].

When an electromagnetic wave hits a dielectric material, it causes electric and magnetic inclusions, which result in dipole moments, which are influenced by relative permittivity and relative permeability [14]. The μ and ε can be classified in the form of the Cartesian coordinate system given in fig.1

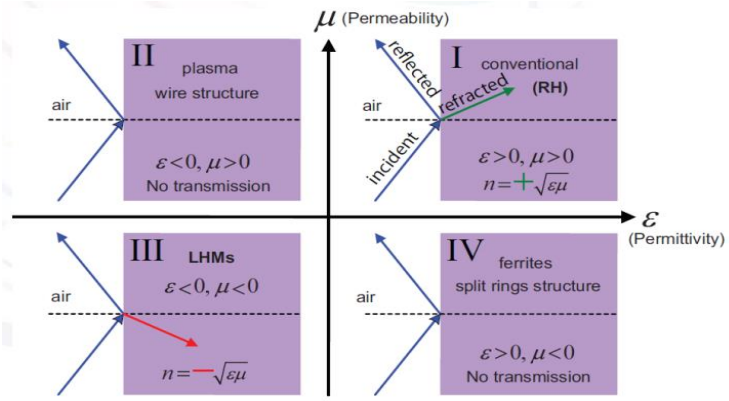

Fig. 1. Classifications of the Relative Permittivity (ε) and relative permeability (μ) [14]

Fig 1 shows the classifications of Relative Permittivity (ε) and relative permeability (μ). The first coordinate shows the Double positive material ($\varepsilon > 0, \mu > 0$), the second coordinate shows the Epsilon negative material ($\varepsilon < 0, \mu > 0$), third coordinate gives the Left-handed Materials ($\varepsilon < 0, \mu < 0$), whereas fourth coordinate shows the Mu negative material ($\varepsilon > 0, \mu < 0$).

(b) Double positive material (DPS)

Most naturally occurring materials (Dielectric materials) fall under this category. According to the Maxwell right-hand thumb rule, if the electric field (E) and magnetic field (H) are perpendicular to each other, then the resultant wave is travelled towards the forward direction (K) when relative permittivity and relative permeability should be positive. So when $\varepsilon > 0, \mu > 0$ then the refractive index should be positive $n=+\sqrt{\varepsilon\mu}$ [14].

(c) Epsilon negative material (ENG)

A medium with negative permittivity and positive permeability can fall under this category. Global metals like gold, silver under infrared region and visible frequencies. D. R smith, in 2006 had proposed the negative permittivity with the Parallel inductor-capacitor circuit (LC).[15] He had successfully verified with the simulation and practical results in the 10GHZ – 20GHZ frequency range, and it does not require the intercell for electrical connectivity. Fig 2 shows the proposed Model for the negative Permittivity by D.R. Smith.

.

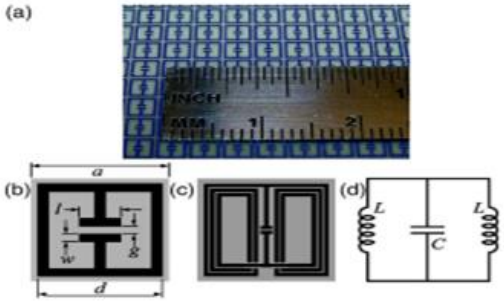

Fig. 2. a) Fabricated sample b) Geometrical design c) multilayer proposed antenna d) Equivalent circuit of the proposed antenna [15]

The fig 2a,fig 2b,fig 2c shows the proposed antenna by D. R. smith with the four balanced split-ring resonators, and fig 2d indicates the equivalent electrical resonating LC circuit with resonance $\omega = \sqrt{\frac{2}{LC}}$

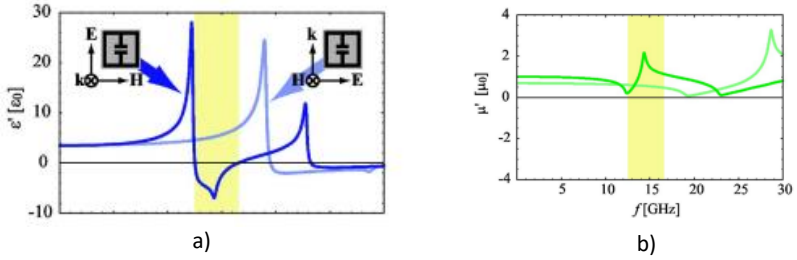

Fig. 3. a) shows the negative permittivity and b) shows the positive permeability [15]

Fig 3a blue line shows the negative permittivity, which falls under yellow color for the 10GHZ-15GHZ region. From the fig 3b shows the positive permeability with green stripes.

(d) Mu Negative material (MNG)

A medium with positive relative permittivity and negative relative permeability ($\varepsilon < 0, \mu < 0$). Gyrotropic, gyromagnetic materials are the best examples of Mu negative materials. Pendry in the year stated that "we can build the artificial magnetic permeability which does not occur with the naturally occurring materials by using the non-magnetic materials loike complementary split-ring resonators.[16] Fig 4 shows the CSRR structures with the simulation results.

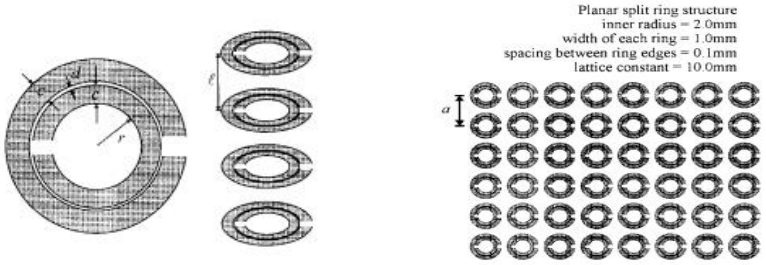

a) b)

Fig. 4. a) Indicates the plain view of the split ring resonators [16]
b) Shows the plain view of the square array of split-ring resonators

Fig 4 shows the realization of relative permeability, which is less than Zero using CSRR structures under Tara Hertz frequency Rang [16]. Pendry had calculated the permeability by considering the infinite conducting cylinders.

The average B-field can be given by

$$B_{avg} = \mu_0 H_0 \qquad (1)$$

Let us consider the H-field overlying entirely outside of the cylinder

$$H_{avg} = H_0 - \frac{\pi r^2}{a^2} j = H_0 - \frac{\pi r^2}{a^2} \frac{-H_0}{\left[1-\frac{\pi r^2}{a^2}\right]+i\frac{2r\sigma}{wr^2\mu_0}}$$

Hence we define

$$\mu_{eff} = \frac{B_{avg}}{\mu_0 H_{avg}} = \frac{1-\frac{\pi r^2}{a^2}+i\frac{2\sigma}{wr\mu_0}}{1+i\frac{2\sigma}{wr\mu_0}} = 1 - \frac{\pi r^2}{a^2}\left[1 + i\frac{2\sigma}{wr\mu_0}\right]^{-1} \qquad (2)$$

For an infinitely conducting cylinder, the above equation shows that the permeability would be greater than zero and less than Zero. We could have replaced the metallic cylinders with prisms of a square cross-section to maximize the volume enclosed within the prism. If the resistivity of the sheets is high, then the additional contribution to μ_{eff} is imaginary, but always less than unity

$$\mu_{eff} \approx 1 + i\frac{\pi r^3 w\mu_0}{2\sigma a^2}\sigma'' wr\mu_0 \qquad (3)$$

(e) Double Negative Materials (DNG)

Pendry had stated that to make the perfect lens artificial materials and which should not be occurred naturally. [9] Later Veselago found that the artificial materials are nothing but the negative permittivity and permeability based on Maxwell relations from the equations 4 and 5 given below [17].

$$\nabla \times E = -j\omega(-\mu)H \Rightarrow \nabla \times E = -j\omega\mu(-H) \qquad \text{-------(4)}$$

$$\nabla \times H = j\omega(-\varepsilon)E \quad \nabla \times (-H) = j\omega(\varepsilon)E \qquad \text{-------(5)}$$

The system is left-handed!

$$K \perp E \perp (-H) \Rightarrow (-K) \perp E \perp (H)$$

E,H and K form a “left handed” system

From equations 4 and 5, Veselago founded that (-k) and E,H are perpendicular to each other, and the resultant wave is propagating towards a backward direction and form Left-handed materials [17].

In the case of plane wave propagation, the electric field and magnetic field can be expressed as

$$E = E_0 e^{(-jkr+jwt)} \quad \text{---------- (6)}$$

$$H = H_0 e^{(-jkr+jwt)} \quad \text{---------- (7)}$$

The pointing vector can be expressed as $S = \frac{1}{2} (E \times H^*)$ ----------(8)

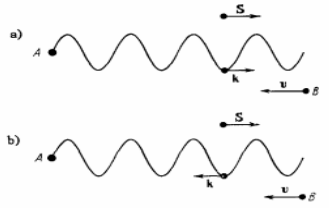

Fig. 5. Propagating wave along the forward and backward direction [9]

A medium with Negative relative Permittivity and Negative relative permeability can be called Double Negative materials. During the international conference 2004, a new name was introduced for an artificial material is METAMATERIAL. Several names were checked to rename the artificial name as Metamaterial, Double negative material, Left-handed media, Media with the negative refractive index, or Backward media [18].

Negative Refractive Index

Veselago stated that the Negative refractive index should be possible only when both permittivity and permeability should be negative [17].

$$n = -\sqrt{\varepsilon\mu} \quad (10)$$

Wounjhang Park states that many advances had been made based on the NIM, which results at the beginning of the New optical material properties[19].

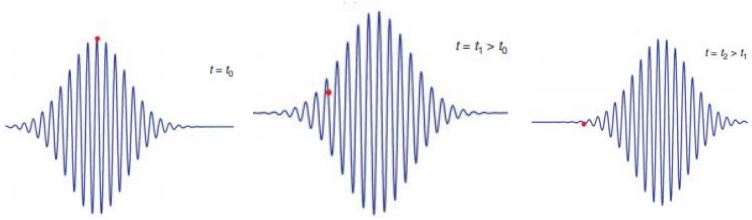

Fig. 6. Gaussian wave propagating in NIM as time passing from t_0 through t_1, t_2[19]

Pendry stated that the Limitations of the General lens could be explained by considering the below equation. The following equation will give the electric component of the field

$$E(r,t) = \sum_{\sigma,k_x k_y} E_\sigma(k_x, k_y) \times \exp(ik_z z + ik_x x + ik_y y - i\omega t)$$

Here they choose the axis is Z-axis and from the Maxwell equations k_z has condition as

$$k_z = +i\sqrt{\omega^2 c^{-2} - k_x^2 - k_y^2}\omega^2 c^{-2} > k_x^2 + k_y^2$$

These evanescent waves can be decaying w.r.t distance, and no phase correction can be restored with the proper amplitude because these propagation waves are limited to

$$k_x^2 + k_y^2 < \omega^2 c^{-2}$$

In order to avoid these limitations, Pendry had placed the parallel slab with the negative refractive index followed by the positive refractive index, which is shown in figure 2.

The reflection coefficient wave is given by

$$\lim_{\mu,\varepsilon\to-1} R_s = \lim_{\mu,\varepsilon\to-1} r + \frac{tt^1 r^1 \exp(2ik_z^1 d)}{1-r^{12}\exp(2ik_z^1 d)} = 0$$

Similarly,a mathematical equation for the P-polarized evanescent waves can be given by

$$\lim_{\mu,\varepsilon\to-1} T_P = \lim_{\mu,\varepsilon\to-1} \frac{2\varepsilon k_z}{\varepsilon k_z + k_z^1}\frac{2k_z^1}{\varepsilon k_z + k_z^1} \text{x} \frac{\exp(ik_z^1 d)}{1-\frac{k_z^1-\varepsilon k_z}{k_z^1+\varepsilon k_z}^2 \exp(2ik_z^i d)} = \exp(-ik_z d)$$

Pendry stated that the "from the above mathematical equations medium does not amplify the evanescent waves and also with a new lens both propagating and evanescent waves can contribute to the resolution of the image" [17].

3 Metamaterials

Over the past few years, the demand for Metamaterial had increased in the scientific communities due to the 5G technology. However, the Metamaterial can also be left-hand, negative refractive index, or backward wave material. A rapid development had been done on the MTM, and the detailed report had been present on the literature review, advantages, and applications of the MTM in this section.

Several advances have been made on the Metamaterials for the antenna's size reduction to increase the radiation efficiency, enhancement in the Bandwidth, and improvement in the Gain [7]. In this section, a literature survey has been discussed. SAMIR SALEM AL-BAWR had proposed a single layer MIMO antenna with the square and Hexagonal shape unit cell at the resonance frequency 28GHZ [20]. He had successfully designed a 3x3 array antenna with negative permittivity and permeability at the given frequency ranges 27 GHz -30GHZ.

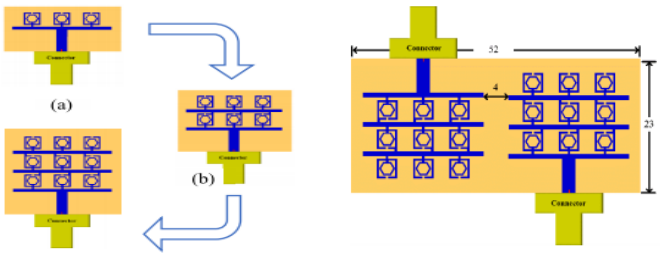

a. b.

c. d.

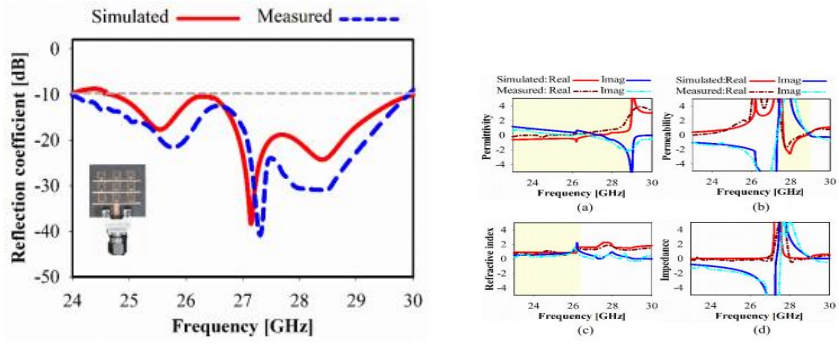

e. f.

Fig. 7. a and b indicates the designed antenna with MIMO, c and d shows the Fabricated antenna, e and f shows the measurements of the proposed antenna

PENG LIU had achieved the good polarization bandwidth by H-shape slot with the characteristic mode analysis and Metamaterials. He had verified the permittivity and permeability of the left-handed materials [21]. In this paper, he had demonstrated the CSRR shaped antenna with the LHM properties by using the FEM method (HFSS) and Matlab [22], another author had designed aerial by using the 7x7 unit square cell, and he achieved the 6.5dB of the Gain with the low Bandwidth [23]. Most research has been going on on the Metamaterials antenna. Metamaterials are in three-dimensional structure so that the fabrication in the bulk quantities may take high lass and complex.

(a) Advantages of Metamaterials

In this section, applications of Metamaterials and advantages havebeen discussed. A metamaterial had been widely used due to its small size with the high radiation efficiency of about 99.9%, high Gain, and polarization Bandwidth.

Pendry stated that the left-handed materials could make the perfect lens, and it can be shown in the fig 8a [1], cloaking and invisibility are also one of the main applications of the MTM, and it can be shown in the fig 8b.[24]. By using the MTM, the aerial can be reduced. [25-28] One of the interesting abilities by the MTM is the phase compensation in the Left-handed media [29,30], if d_1 is the thickness and $n_i$is the refractive index of the RHM and d_2 is the thickness, and n_2 is the refractive index of the LHM then it proved that the Zero phase compensation iff$yd_1/d_2 = |n2|/|n1|$

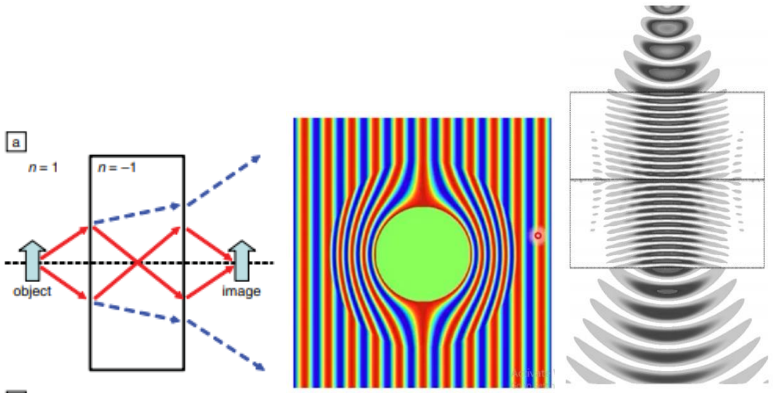

a) b) c)

Fig. 8. a) perfect lens by the MTM
b) Clocking and invisibility
c) Phase compensation

(b) Applications of the Metamaterial

The MTM can be used in a variety of devices and hypotheses due to its unique properties. MTM wit h filter, absorbersand 5G communications are the core three applications of the MTM.

From the last few years,Metamaterial with a 5G antenna has been one of the promising areas, and table 1 shows the different literature reviews of the 5G antenna using MTM.

Table 1 shows the comparison of the designed antennas from the different research papers. Tayyab Shabbir had designed a fractal shape antenna with the 300MHZ Bandwidth [31] Arshad K. Vhad proposed the MIMO antenna with the 1GHZ of Bandwidth under sub 6GHZ band [32], it observe the good Gain with 7.4dbi[33].

Table 1: Comparison of the different research papers on 5G antenna using MTM

Ref No	The shape of the patch	No of Ports	Dielectric Material	Size of antenna	Bandwidth	Frequency Range	Gain	Refractive index
31	Fractal slotted rectangular patch with the dual feeding	16	FR4 (4.4)	22mmX20mmx1.5mm of each patch	300MHZ	3.65-3.35GHZ	6.5dbi	Near Zero (-0.18)
32	2x2 MIMO antenna with the inverted s shape patch	4	FR4 (4.4)	70mmx73.7mmx1.6mm	1GHZ	3-4GHZ	-	-
33	Stair case rectangular patch antenna with dual substrate	1	RT(2.2)	30mmx30.5mmx1.31mm	- (No lower bands and upper band at 27.5ghz)	24.25 - 27.5 GHZ	7.4dbi	-

34	L-shape patch antenna	1	RT(2.2)	12mmx16 mmx0.25 4mm (Reconfig urable antenna)	700MHZ (approximat ely)	28-29GHz	1.7db & 1.5db	Positive And negative
35	1x2 Array rectangular patch with the SRR	1	FR4 (4.4)	8mmx8m mx1.6 mm	1600MHZ 600MHZ	25-26.6GH Z 33-33.6GH Z	4.01d b 3.33d b	-
36	cylinder shaped CSRR	1	RT(2.2)	3mmx44 mm0.43m m	41GHZ	3-44GHZ	-	-
37	Rectangular patch antenna with the dual substrate	1	FR4 (4.4)	136mmx6 8mmx1m m	200MHZ	4.55-4.75GH Z	-	-
38	Multiple slots and dual substrate with the Flaquet mode analysis	Flaqu et port	RogeressT MM (9.2)	-	14.75GHZ	22-34GHZ	-	Negativ e

Table 2: Comparison of the different research papers on filters using MTM

Ref no	**Shape Of Patch**	**No Of Ports**	**Dielectric Material**	**Size of antenna**	**Bandw idth**	**Freque ncy Range**	**Gain**	**Filter**	**Any other results**
39	Square shape patch and t-shape shape slots with dual feeding technique	2	RT(2.2)	83x120x1. 575mm	80MHZ	80MHZ	-	Chebysh ev filter (3 poles) Quasi elliptical (4 pole)	-
40	square shape patch with the multilayer antenna	5x5	-	-	-	500THZ	-	-	Electric field 1.06e+07
41	CSRR with the Dual feeding structure	2	RT(2.2)	26x30x1.5 75mm	50MHZ	--	-	Bandpas s filter	Q-factor at 1.55ghz and 2.70ghz and 3.65GHz is 14.09,30, 36
42	circular slots	1	-	-	-	-	-	-	Band

	with the E-shaped patch antenna								structure of SV modes
43	Rectangular patch with the silicon substrate	1	n-type silicon (11.58)	-	-	0.1-2THZ	-	LPF	Cut off frequencies varies from 0.58 to 1.74THZ
44	square shape patch antenna with the inverted s-shape slots	2	Rogers 3003(3)	7x18x1.52 mm	-	0-8GHZ	-	LPF	Cut of frequency at 8GHZ
45	Inverted s-shape slots with the dual feeding	2	FR4(4.4)	20.9x15.3 x1.6mm	Maximum 100MHZ	2GHZ,4.25GHZ 5.26GHZ	-	Bandpass Filter	Group delay
46	Rectangular patch with the dual feeding	2	Rogers 5870(2.2)	45x15x0.787mm	8.5GHz	2-10GHZ	-	Notch band Filter (4.5GHZ-6GHZ)	-
47	Rectangular slots patch antenna with the Dual feeding	2	Rogers 6010(10.2)	16x16x1.27mm	2.18-2.32GHZ	140MHZ	-	Bandpass filter	Plotted the phase with a frequency graph

Bashar A designed an antenna with the l-shape antenna, and also they had successfully verified the MTM properties [34]. Later several researchers had worked for the MTM under 5G applications, and the maximum they had been attained was 14.5GHZ of Bandwidth, but none of them had verified the Negative Permittivity and negative permeability with the refractive index values [35-38].By designing the filter with the normal microstrip patch antenna has been facing more difficulty like narrow Bandwidth and less efficiency and size of the antenna is also more. Table 2 shows the comparison of the different research work from the last decade.

In Isaias, Zagoya-Mellado had designed an antenna with the square patch for quasi elliptical filter [39]. In this paper, the author had designed an antenna for the Bandpass filter and achieved a good Q-factor under 1.5 to 14.09 MHZ [41]. Inverted s-shape with dual feeding and rectangular patch with the dual feeding had been designed for the Bandpass filter applications [45,47]. A notch filter had designed with 2-10GHZ of the frequency range [46].

It was founded that a tremendous development in the field of absorbers using the Metamaterial, i.e., absorption radiation efficiency is 98%. Table 3 shows the comparison table of the different research papers on Metamaterial using absorbers.

Table 3: Comparison of the MTM with absorber for the different research papers

Ref no	**The shape of the patch**	**No of ports**	**Size of the antenna**	**MTM Absorption Frequency Range**	**No of absorption peaks**	**Bandwidth**	**Other results**
48	Star-shaped patch	Floquet port	13x13x0.217mm	20-60GHZ	3	-	Absorption rate 99.89%
49	Rectangular shape patch antenna	Floquet port	-	1-3THZ	1	-	-
50	circular shape SRR with plus shape slot	Floquet port	7mm of radius	0-18GHZ	-	8GHZ	-
51	Circular and square shape patch antenna with three layers	Floquet port	$0.0925\lambda_0 \times 0.0925\lambda_0$ at 10.28 GHz.	0-12GHZ	1	-	Absorption rate 97.5%
52	Circular split ring resonators	Floquet port	-	7.25-12GHZ	1	4GHZ	-
53	Double layer DCRR type absorber	4 port	72.136x34.036x0.762 mm	2.6-4GHZ	3	-	-
54	Ring-type metamaterial absorber	Floquet port	-	4.5-7.0GHZ	3	800MHZ	-
55	Bidirectional metamaterial absorber	Floquet port	-	4-5.5GHZ	-	-	-
56	Rectangular slots with the double substrate	Floquet port	-	2-11GHZ	3	-	-
57	Wheel shaped circular patch antenna	Floquet port	20x20x18 mm	1-4GHZ	-	2GHZ	-
58	AD-CRR type metamaterial absorber	Floquet port	72.136x34.03x1.5mm	2.5-2.9GHZ	1	100MHZ	-

59	T-shape slots with multilayer patch antenna	Floquet port	-	6.6-8.9THZ	1	2.3GHZ	-
60	MDCRR unit cell	Floquet port	-	4-11GHZ	3	50MHZ	-

It is very difficult to design an aerial for the perfect absorber with the normal patch antenna. Minyeong Yoo, Hyung Ki Kim,Sungjoon Lim had designed an antenna and achieved a 97.3% absorption rate [51]. Evren Ekmekci, Esra Demir had achieved the three absorption peaks with Double-layer substrate [53]. Huiqing Zhai, a Member, had designed an aerial with the double layer RT Duriod substrate material and achieved three absorptions peaks [56].

(c) Limitations of the MTM

Due to certain advantages with the MTM, which are stated in the previous section, there are certain disadvantageswith MTM like they are 3D in nature a bulk production may not be possible, the shape of the antenna may be changed during their operation [61].

4 Metasurface

Metasurface is two-dimensional with a planar structure. Due to their planar structures, it is easy to fabricate, and losses are also very less when compare to the MTM.[62]. It is one of the promising technology in electromagnetic and optics, as shown in fig 9 [63].

Fig. 9. Metasurface [62]

Md Rezwanul Ahsan had proposed a multilayer radiating circular patch for the enhancement of the Bandwidth and Gain as shown in fig 10 [64]; another author had fabricated octal shaped EBG antenna with the Bandwidth of the 200MHZ of dimensions 150mmx150mmx1.6mm as shown in fig 10 [65]. Sarawuth CHAIMOOL had successfully simulated a 4x4 split ring resonator with the 9.2dBi and 340MHZ of Bandwidth; Yijun Feng had proposed an aerial for the phase compensation using coaxial cable as shown in fig 10 [66], Metasurfacehas a good phase compensation even the patch length varies [67].

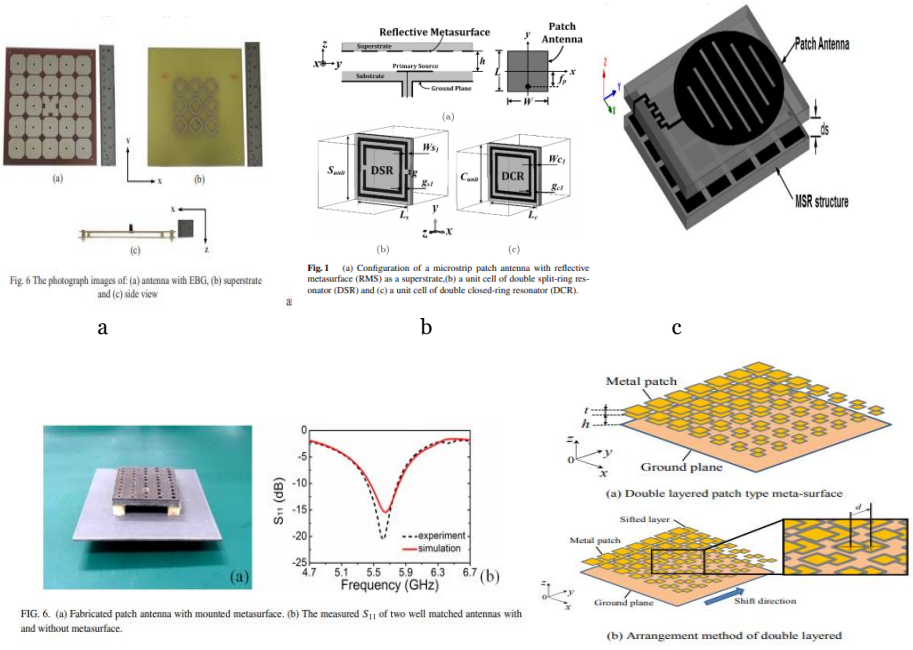

Fig. 6 The photograph images of: (a) antenna with EBG, (b) superstrate and (c) side view

Fig. 1 (a) Configuration of a microstrip patch antenna with reflective metasurface (RMS) as a superstrate,(b) a unit cell of double split-ring resonator (DSR) and (c) a unit cell of double closed-ring resonator (DCR).

FIG. 6. (a) Fabricated patch antenna with mounted metasurface. (b) The measured S_{11} of two well matched antennas with and without metasurface.

a b c

d e

Fig. 10. Designs from the various literatures reviews[64,65,66,67]

(a) Advantages of Metasurface

As the Metasurface is a two-dimensional antenna, it is very easy to fabricate and low cost. It has a special property that it can control the pattern and has a unique polarization. Due to its simple structure, it has low losses, and it can achieve 99% of the Radiation efficiency and high Gain and Bandwidth [68].

(b) Applications of the Metasurface

Due to the 2D in structure, the MTS has a lot of advantages over the Metamaterial; it is one of the booming technologies for the 5G and for several applications. Metasurface has a lot of applications such as Millimeter-wave applications, 5G, wireless power transmissions, and Wireless energy harvesting systems.

Table 4: Comparison table for the Metasurface using 5G antennas on different research papers

Ref No	The shape of the patch	No of Ports	Size of antenna	Bandwidth	Frequency Range	Gain
69	Hexagonal shaped antenna on one substrate and square type slots on the lower substrate with coaxial feeding	4x4 array	$1.1\lambda_o \times 1.1\lambda_o \times 0.093\lambda_o$.	10GHZ	24-34.1GHZ	11dbic
70	4x4 MIMO antenna with the square slots	2x2 array	$1.58\lambda_o \times 1.58\lambda_o \times 0.068\lambda_o$.	1.44GHZ	4.41–5.85 GHz	8.4dbi

	on both the substrates with the coaxial feeding					
71	3x3 MIMO antenna with the square slots and by using dual substrates	3x3 array	95mmx95mmx2.66mm	1GHz	4.4-5.4GHZ	12.8dbi
72	cylindrical shaped patch antenna with the hallow type of structure of the antenna by using six-port coaxial feeding	1	60x60x7.92mm	3.1GHZ 1.6GHZ	3.1-6.2GHZ 7.1-8.7GHZ	7.4±1.5dbi
73	Square slots with the dual substrate structure	8x8	$10\lambda_0 \times 10\lambda_0 \times 5\lambda_0$	800MHZ	5-6GHZ	3.3db
74	square shape patch antenna with the circular slots	1	17.5mmx8mmx0.8mm	200MHZ	28GHZ	-
75	Multiple (six) layer antenna with bow shape patch	1	80mmx80mm	2.02GHZ	1.69-3.69GHZ	5.14±1.24 dbi
76	Hexagonal shape patch with the square slots by using coaxial feeding structure	1	$1.0\lambda_0 \times 1.0\lambda_0 \times 0.04\lambda_0$	4.6GHZ	25-29.6GHZ	11dbic

Niamat Hussain had designed an antenna with the 10GHZ with the low Gain of 11dbic [69]. Another author MIMO aerial had been designed and achieved 1.44GHZ of Bandwidth [70]. Later very few researchers had worked on the MTS with the 5G aerial and attain 4.6GHZ of bandwidth Maximum [71-76]

Table 5: Comparison table for the Metasurface with filter in different research papers

Ref no	**Shape of patch**	**No of ports**	**Size of antenna**	**Bandwidth**	**Frequency Range**	**Gain**	**Filter**
77	2x2 MIMO antenna with the square shape patch antenna	2x2	33x33x1.778mm	2GHZ	6.4-8.4GHZ	8dbi	BPF (6.4-8.4) GHZ
78	square slot with the line feeding technique	1	78x78x3.813mm	1.8GHZ	4.2-6GHZ	8dbi	BPF (4.2-6) GHZ
79	Color filtering restoring using Si:H Metasurface	Flaquet port	40μmx40μmx80nm	-	450 nm to 1650 nm	-	Colour filtering

80	Metasurface structure capable of filtering light of a specific wavelength range	Flaquet port	-	-	-	-	Colour filtering
81	Reflection and transmission mode dielectric color filters design	Flaquet port	-	-	-	-	Colour filtering
82	Schematic drawing of the proposed band stop filter	Flaquet port	240x160x0.9mm	129GHZ	371-500GHZ		Bandstop filter
83	Rectangular shaped absorber	-	20.4cmx20.4cmx0.49mm	-	1.8-6	-	Bandpass filter
84	Multilayered aluminum-based Metasurface	-	-	-	-	-	-
85	Schematic of Ultrathin filter	-	-	6.4 THZ	2-8THZ	-	Band Stop filter
86	Single-layer Metasurface	-	--	500nm	400-800nm	--	-
87	A Metasurface made of chains of I-CSRRs	-	-	-	-	-	Bandpass filter
88	Configuration of the double layer filtering cloak coating surrounding a monopole.	-	-	50MHZ	-	-	-

It was observed that the lowerBandwidth for the Metamaterial using filters with the Lower cut-off frequency and also designing of the antenna is quite complex. Table 5 shows the comparison table for Metasurface with filters over the different research papers. Table 6 shows the comparison of the literature review of the different research papers in the Metasurface with absorbers.

Table 6: Comparison table literature review of Metasurface with absorbers

Ref no	**The shape of the patch**	**Size of the antenna**	**MTM Absorption Frequency Range**	**No of absorption peaks**	**Bandwidth**	**Fabricated Model**	**Other results**
89	Square patch antenna for perfect absorber	-	4-20GHZ	-	-	-	-
90	Rectangular shape antenna	-	-	1	-	--	-

91	Reactive impendence	-	1-3GHZ	-	50MHZ	-	
92	MTS absorber with slow-wave effect	35mmx15mm x2mm	5-8GHZ	-	50MHZ	-	-
93	Periodic cell with the metamaterial absorber	Height of substrate 3mm	8.2-12.4GHZ	1	3GHZ	YES	90% absorption efficiency
94	Reflection of the Si resonators array on the quartz	-	0.6-2.2 μm	3(0.641-0.665 μm)	-	-	98% absorption efficiency
95	Si-based metasurface absorber	Height of the substrate = 300nm	0.6-1.0 μm	3(0.655,0.677 μm,0.823 μm)	-	-	99% absorption efficiency
96	Plus shaped met surface absorber	-	9-14 μm	3(8-13 μm)	-	-	-

It was observed that the Metasurface with filter had been designed with the maximum Bandwidth of 1.8 GHZ and Gain is 8.2dBi.For the Metasurface with the 5g antenna, most of the researchers had designed under Microwave frequencies with the maximum frequency is 10GHZ. For the Metasurface absorbers, it was observed that the maximum three absorption peaks under the Wavelength range of 0.6-2.2 μm. From all the above earlier researchers, it was founded that very few of them had verified the MTM property and their fabricated Model.

5 Conclusion

The purpose of this review paper is to discuss the basics of the left-handed material, limitations and silent features of the Metamaterial, and finally, recent advancements made in the field of the Metasurface.Pendry stated that the perfect lens could be made by using artificial materials. Veselago found that the artificial materials have nothing but the negative of relative permittivity and permeability, and the resultant propagated wave is travel along the backward direction. A high bandwidth, gain, and good radiation efficiency can be achieved with the LHM. Metamaterials are three dimensional in nature so, it is complex in a structure whereas Metasurface is two dimensional it is simplex in structure and easy to fabricate. MTS can be used in cloaking and invisibility devices to make a perfect lens. It has the special properties of phase compensation. A lot of inventions would be taken place in the future communications and imaging devices.Despite the fact that much successful work on metasurfaces has been done in the microwave regime, the use of metasurfaces in the Design of future communication and imaging devices is still an area with a lot of room for research and development.

Future work

Due to Metamaterial in 3D in nature, it is challenging in bulk quantity. By using Metamaterial, there is a possibility to reduce the backward radiation, and the antenna's Gain can be increased with the Metasurface antenna.

References

[1] Paul, L. C. et al. (2016). Performance analysis of cut feed rectangular microstrip patch antenna by varying feeder length and width. In *3rd International Conference on Electrical, Electronics, Engineering Trends, Communication, Optimization and Sciences,* 1-4.

[2] Reddy, S. M. et al. (2018). Comparative Analysis of Edge Feeding and coaxial Feeding Technique with Fixed Frequency. *International Journal of Engineering & Technology*, 7(2.7):848-853.

[3] Reddy, S. M. et al. (2018). Microstrip Line Fed Fractal Monopole Antenna with Defected Ground Structure. *International Journal of Engineering & Technology*, 7(3.31): 21-24.

[4] Shaban, H. F., Elmikaty, H. A. and Shaalan, A. (2008). Study the effects of electromagnetic band-gap (EBG) substrate on two patch microstrip antenna. *Progress In Electromagnetics Research B*, *10*:55-74.

[5] Thakare, Y. B. (2010). Design of fractal patch antenna for size and radar cross-section reduction. *IET microwaves, antennas & propagation*, 4(2): 175-181.

[6] Swathi, S., Ujjwal, G. and Chilukuri, S. (2018). A Frequency Reconfigurable Antenna with slotted ground plane for Multi-band Applications. In *IEEE Indian Conference on Antennas and Propogation,* 1-5.

[7] Kumar, M. V. et al. (2019). Stair Plus Rectangular Patch CPW Feeding Antenna with UltraWide Band. *Journal of Advanced Research in Dynamic and Control Systems*, 11(02): 1409–1420.

[8] Kumari, E. K. and Kumar, M. V. (2019). A Triple band Microstrip Antenna with Enhanced Bandwidth for Radar Applications. (2019). *International Journal of Recent Technology and Engineering*, 8(2S11): 975–978.

[9] Pendry, J. B. (2000). Negative refraction makes a perfect lens. *Physical review letters*, *85*(18): 3966.

[10] Kshetrimayum, R. S. (2004). A brief intro to metamaterials. *IEEE potentials*, *23*(5): 44-46.

[11] Luo, X. et al. (2015). Taming the electromagnetic boundaries via metasurfaces: from theory and fabrication to functional devices. *International Journal of Antennas and Propagation*, 2015: 204127.

[12] Bukhari, S. S., Vardaxoglou, J. Y. and Whittow, W. (2019). A metasurfaces review: Definitions and applications. *Applied Sciences*, 9(13): 2727.

[13] Faenzi, M. et al. (2019). Metasurface antennas: new models, applications and realizations. *Scientific reports*, 9(1): 1-14.

[14] Markoš, P. and Soukoulis, C. M. (2003). Left-Handed Materials. In B. A. van Tiggelen & S. E. Skipetrov (Eds.), *Wave Scattering in Complex Media: From Theory to Applications* (pp. 308–329). Springer Netherlands.

[15] Schurig, D. R. S. D., Mock, J. J. and Smith, D. R. (2006). Electric-field-coupled resonators for negative permittivity metamaterials. *Applied physics letters*, *88(*4): 041109.

[16] Pendry, J. B. et al. (1999). Magnetism from conductors and enhanced nonlinear phenomena. *IEEE transactions on microwave theory and techniques*, 47(11): 2075-2084.

[17] Veselago, V. G. (1968). THE ELECTRODYNAMICS OF SUBSTANCES WITH SIMULTANEOUSLY NEGATIVE VALUES OF AND μ. *Soviet Physics Uspekhi*, 10(4): 509.

[18] Ziolkowski, R. W. and Heyman, E. (2001). Wave propagation in media having negative permittivity and permeability. *Physical review E*, 64(5): 056625.

[19] Park, W. and Kim, J. (2008). Negative-index materials: Optics by design. *MRS bulletin*, 33(10): 907-914.

[20] Al-Bawri, S. S. et al. (2020). Hexagonal shaped near zero index (NZI) metamaterial based MIMO antenna for millimeter-wave application. *IEEE Access*, 8: 181003-181013.

[21] Liu, P. et al. (2020). Broadband and low-profile penta-polarization reconfigurable metamaterial antenna. *IEEE Access*, 8: 21823-21831.

[22] Feng, B. K. (2006). *Extracting material constitutive parameters from scattering parameters*. NAVAL POSTGRADUATE SCHOOL MONTEREY CA.

[23] Zhou, X. and Zhao, X. P. (2007). Resonant condition of unitary dendritic structure with overlapping negative permittivity and permeability. *Applied Physics Letters*, 91(18): 181908.

[24] Singh, G. and Marwaha, A. (2015). A review of metamaterials and its applications.

[25] Raval, F. et al. (2013). Design & implementation of reduced size microstrip patch antenna with metamaterial defected ground plane. In *International Conference on Communication and Signal Processing,* 186-190.

[26] Rajab, K. Z., Mittra, R. and Lanagan, M. T. (2005). Size reduction of microstrip antennas using metamaterials. In *IEEE Antennas and Propagation Society International Symposium,* 2: 296-299.

[27] Gunung, M. A. and Munir, A. (2011). Size reduction of compact dual-band antenna based on metamaterials. In *6th International Conference on Telecommunication Systems, Services, and Applications,* 204-208.

[28] Agrawal, A. and Garg, N. K. (2015). Reduction in the size of rectangular microstript patch antenna. *International Research Journal of Engineering and Technology*, 2(02).

[29] Engheta, N. and Ziolkowski, R. W. (2005). A positive future for double-negative metamaterials. *IEEE Transactions on microwave theory and techniques*, 53(4): 1535-1556.
[30] Wang, J. et al. (2020). Metantenna: When metasurface meets antenna again. *IEEE Transactions on Antennas and Propagation*, 68(3): 1332-1347.
[31] Shabbir, T. et al. (2020). 16-port non-planar MIMO antenna system with near-zero-index (NZI) metamaterial decoupling structure for 5G applications. *IEEE Access*, 8: 157946-157958.
[32] Karimbu V. A. et al. (2020). Compact material Based 4 × 4 Butler Matrix With Improved Bandwidth for 5G Applications. *IEEE Access*.
[33] Jiang, H. et al. (2019). A symmetrical dual-beam bowtie antenna with gain enhancement using metamaterial for 5G MIMO applications. *IEEE Photonics Journal*, 11(1): 1-9.
[34] Esmail, B. A. et al. (2021). Reconfigurable metamaterial structure for 5G beam tilting antenna applications. *Waves in Random and Complex Media*, 31(6): 2089-2102.
[35] Ali, T. et al. (2018). A Dual band Metamaterial Antenna for 5G and Higher Satellite band Applications. In *4th International Conference for Convergence in Technology,* 1-4.
[36] Thanuj, D. et al. (2018). Metamaterial based compact planar antenna for UWB and 5G applications. In *2nd International Conference on Micro-Electronics and Telecommunication Engineering,* 33-35.
[37] Xu, S. et al. (2017). Anisotropic metamaterial based decoupling strategy for MIMO antenna in mobile handsets. In *International Workshop on Antenna Technology: Small Antennas, Innovative Structures, and Applications,* 34-37.
[38] Sansa, I., Nasri, A. and Zairi, H. (2019). A miniaturized metamaterial unit cell for 5G applications. In *IEEE 19th Mediterranean Microwave Symposium,* 1-4.
[39] Zagoya-Mellado, I., Corona-Chavez, A. and Llamas-Garro, I. (2009). Miniaturized metamaterial filters using ring resonators. In *IEEE MTT-S International Microwave Workshop Series on Signal Integrity and High-Speed Interconnects*, 45-48.
[40] Ahamed, E. et al. (2020). Digital metamaterial filter for encoding information. *Scientific reports*, 10(1): 1-9.
[41] Alam, M. J. et al. (2019). Left-handed metamaterial bandpass filter for GPS, Earth Exploration-Satellite and WiMAX frequency sensing applications. *PloS one*, 14(11): e0224478.
[42] Zhu, H. and Semperlotti, F. (2013). Metamaterial based embedded acoustic filters for structural applications. *AIP Advances*, 3(9): 092121.
[43] Zhu, Z. et al. (2013). A metamaterial-based terahertz low-pass filter with low insertion loss and sharp rejection. *IEEE Transactions on Terahertz Science and Technology*, 3(6): 832-837.
[44] Kurhe, N. M. and Labade, D. R. P. (2018). *Design of Low Pass Filter for Ultra Wide Applications Using Metamaterial Structures*. 6.
[45] Choudhary, D. K. and Chaudhary, R. K. (2018). A compact triple band metamaterial inspired bandpass filter using inverted S-shape resonator. *Radioengineering*, 27(2).
[46] Ali, A. and Hu, Z. (2008). Metamaterial resonator based wave propagation notch for ultrawideband filter applications. *IEEE Antennas and Wireless Propagation Letters*, 7: 210-212.
[47] Choudhary, D. K. and Chaudhary, R. K. (2017). A miniaturized two pole metamaterial bandpass filter using Ω-shaped IDC for cellular application. In *IEEE MTT-S International Microwave and RF Conference,* 283-286.
[48] Wang, N. et al. (2015). Novel Quadruple-Band Microwave Metamaterial Absorber. *IEEE Photonics Journal*, 7(1): 1–6.
[49] Wang, B. X. et al. (2015). Polarization Tunable Terahertz Metamaterial Absorber. *IEEE Photonics Journal*, 7(4): 1–7.
[50] Sharma, A., Panwar, R. and Khanna, R. (2019). Experimental Validation of a Frequency-Selective Surface-Loaded Hybrid Metamaterial Absorber with Wide Bandwidth. *IEEE Magnetics Letters*, 10: 1–5.
[51] Yoo, M., Kim, H. K. and Lim, S. (2016). Angular- and Polarization-Insensitive Metamaterial Absorber Using Subwavelength Unit Cell in Multilayer Technology. *IEEE Antennas and Wireless Propagation Letters*, 15: 414–417.
[52] Ahmed, F., Hassan, T. and Shoaib, N. (2020). An Ultrawideband Ultrathin Metamaterial Absorber Based on Circular Split Rings. *IEEE Antennas and Wireless Propagation Letters*, 19(3): 512–514.
[53] Ekmekci, E. and Demir, E. (2016). On/Off Switching of Absorption Spectra by Layer Shifting for Double-Layer Metamaterial-Based Absorber. *IEEE Antennas and Wireless Propagation Letters*, 15: 532–535.
[54] Ren, J., Gong, S. and Jiang, W. (2018). Low-RCS Monopolar Patch Antenna Based on a Dual-Ring Metamaterial Absorber. *IEEE Antennas and Wireless Propagation Letters*, 17(1): 102–105.
[55] Costa, F. et al. (2013). Low-cost metamaterial absorbers for sub-GHz wireless systems. *IEEE Antennas and Wireless Propagation Letters*, 13: 27-30.
[56] Zhai, H. et al. (2014). A triple-band ultrathin metamaterial absorber with wide-angle and polarization stability. *IEEE Antennas and Wireless Propagation Letters*, 14: 241-244.
[57] Banadaki, M. D., Heidari, A. A. and Nakhkash, M. (2017). A metamaterial absorber with a new compact unit cell. *IEEE Antennas and Wireless Propagation Letters*, 17(2): 205-208.
[58] Al-Badri, K. S. et al. (2016). Monochromatic tuning of absorption strength based on angle-dependent closed-ring resonator-type metamaterial absorber. *IEEE Antennas and Wireless Propagation Letters*, 16: 1060-1063.
[59] Zhang, Y. et al. (2020). Study on temperature adjustable terahertz metamaterial absorber based on vanadium dioxide. *IEEE Access*, *8*: 85154-85161.

[60] Singh, A. K., Abegaonkar, M. P. and Koul, S. K. (2018). Dual-and triple-band polarization insensitive ultrathin conformal metamaterial absorbers with wide angular stability. *IEEE Transactions on Electromagnetic Compatibility*, 61(3): 878-886.
[61] Holloway, C. L. et al. (2012). An overview of the theory and applications of metasurfaces: The two-dimensional equivalents of metamaterials. *IEEE Antennas and Propagation Magazine*, 54(2): 10-35.
[62] Bukhari, S. S., Vardaxoglou, J. Y. and Whittow, W. (2019). A metasurfaces review: Definitions and applications. *Applied Sciences*, 9(13): 2727.
[63] Luo, X. et al. (2015). Taming the electromagnetic boundaries via metasurfaces: from theory and fabrication to functional devices. *International Journal of Antennas and Propagation*, *2015*.
[64] Ahsan, M. R. et al. (2015). Metasurface reflector (MSR) loading for high performance small microstrip antenna design. *PloS one*, 10(5): e0127185.
[65] Arnmanee, P. (2018). Gain Improvement of Microstrip Patch Antenna using Octagonal-Loop Metasurface Superstrate and Octagonal-Shaped EBG Structure. In *15th International Conference on Electrical Engineering/Electronics, Computer, Telecommunications and Information Technology,* 21-24.
[66] Chaimool, S., Chung, K. L. and Akkaraekthalin, P. (2010). Bandwidth and gain enhancement of microstrip patch antennas using reflective metasurface. *IEICE transactions on communications*, 93(10): 2496-2503.
[67] Chen, K. et al. (2015). Improving microwave antenna gain and bandwidth with phase compensation metasurface. *AIP advances*, 5(6): 067152.
[68] Faenzi, M. et al. (2019). Metasurface antennas: new models, applications and realizations. *Scientific reports*, 9(1): 1-14.
[69] Hussain, N. et al. (2020). A metasurface-based low-profile wideband circularly polarized patch antenna for 5G millimeter-wave systems. *IEEE Access*, 8: 22127-22135.
[70] Nie, N. S. et al. (2019). A low-profile wideband hybrid metasurface antenna array for 5G and WiFi systems. *IEEE Transactions on Antennas and Propagation*, 68(2): 665-671.
[71] Li, T. and Chen, Z. N. (2018). Metasurface-Based Shared-Aperture 5G ${S} $-/${K} $-Band Antenna Using Characteristic Mode Analysis. *IEEE Transactions on Antennas and Propagation*, 66(12): 6742-6750.
[72] Feng, B. et al. (2018). A Dual-Wideband and High Gain Magneto-Electric Dipole Antenna and Its 3D MIMO System With Metasurface for 5G/WiMAX/WLAN/X-Band Applications. *IEEE Access*, 6: 33387–33398.
[73] Li, S. et al. (2020). Characterization of metasurface lens antenna for sub-6 GHz dual-polarization full-dimension massive MIMO and multibeam systems. *IEEE Transactions on Antennas and Propagation*, 68(3): 1366-1377.
[74] Nair, P. S., Patnaik, A. and Kartikeyan, M. V. (2018, December). Multi-band SIW antenna with modulated metasurface at 5G frequency. In *IEEE Indian Conference on Antennas and Propogation,* 1-4.
[75] Lai, J. et al. (2017). A substrate integrated magneto-electric dipole antenna using metasurface for 2G/3G/LTE/5G applications. In *Sixth Asia-Pacific Conference on Antennas and Propagation,* 1-3.
[76] Hussain, N. et al. (2020). Metasurface-based single-layer wideband circularly polarized MIMO antenna for 5G millimeter-wave systems. *IEEE Access*, 8: 130293-130304.
[77] Yang, W. et al. (2018). Novel filtering method based on metasurface antenna and its application for wideband high-gain filtering antenna with low profile. *IEEE Transactions on Antennas and Propagation*, 67(3): 1535-1544.
[78] Pan, Y. M. et al. (2016). A low-profile high-gain and wideband filtering antenna with metasurface. *IEEE Transactions on Antennas and Propagation*, 64(5): 2010-2016.
[79] Park, C. S. et al. (2017). Structural color filters enabled by a dielectric metasurface incorporating hydrogenated amorphous silicon nanodisks. *Scientific reports*, 7(1): 1-9.
[80] Han, X. et al. (2021). Inverse design of metasurface optical filters using deep neural network with high degrees of freedom. *InfoMat*, 3(4): 432-442.
[81] Panda, S. S., Vyas, H. S. and Hegde, R. S. (2019). All-dielectric metasurfaces for reflection and transmission-mode color filter arrays. In *Workshop on Recent Advances in Photonics,* 1-3.
[82] Deng, H., Chan, M. and Zhou, S. (2019). Terahertz broadband band-stop filter based on metasurface. In *IEEE International Conference on Electron Devices and Solid-State Circuits,* 1-3.
[83] Ortiz, J. D. et al. (2013). Self-complementary metasurface for designing narrow band pass/stop filters. *IEEE microwave and wireless components letters*, 23(6): 291-293.
[84] Soni, A., Purohit, S. and Hegde, R. S. (2016). Multilayered aluminum plasmonic metasurfaces for ultraviolet bandpass filtering. *IEEE Photonics Technology Letters*, 29(1): 110-113.
[85] Liu, J. Y., Huang, T. J. and Liu, P. K. (2018). Tunable polarization-independent terahertz band-stop filter based on graphene metasurface. In *43rd International Conference on Infrared, Millimeter, and Terahertz Waves,* 1-2.
[86] Yang, C. et al. (2019). All-dielectric metasurface for highly tunable, narrowband notch filtering. *IEEE Photonics Journal*, 11(4): 1-6.
[87] Ortiz, J. D. et al. (2014). Metasurfaces for angular filtering and beam scanning. In *8th International Congress on Advanced Electromagnetic Materials in Microwaves and Optics,* 34-36.
[88] Jiang, Z. H. and Werner, D. H. (2015). An integrated metasurface filtering cloak for monopole antennas. In *IEEE International Symposium on Antennas and Propagation & USNC/URSI National Radio Science Meeting*, 55-56.

[89] Zhou, S. N., Wang, Z. B. and Feng, Y. J. (2012). Optimal design of wideband radar absorbing structure consisting of resistive meta-surface layers. In *International Conference on Microwave and Millimeter Wave Technology,* 5: 1-4.
[90] Alaee, R., Albooyeh, M. and Rockstuhl, C. (2017). Theory of metasurface based perfect absorbers. *Journal of Physics D: Applied Physics*, 50(50): 503002.
[91] Mosallaei, H. and Sarabandi, K. (2005). A one-layer ultra-thin meta-surface absorber. In *2005 IEEE Antennas and Propagation Society International Symposium,* 1: 615-618.
[92] Li, Z. et al. (2020). A metasurface absorber based on the slow-wave effect. *AIP Advances*, 10(4): 045311.
[93] Gogoi, D. J. and Bhattacharyya, N. S. (2018). Metasurface absorber based on water meta "molecule" for X-band microwave absorption. *Journal of Applied Physics*, 124(7): 075106.
[94] Liu, G. et al. (2018). Hybrid metal-semiconductor meta-surface based photo-electronic perfect absorber. *IEEE Journal of Selected Topics in Quantum Electronics*, 25(3): 1-7.
[95] Liu, Z. et al. (2020). Silicon antennas metasurface based light absorber with quantitatively adjustable operating frequency and intensity. *IEEE Journal of Selected Topics in Quantum Electronics*, 27(1): 1-6.
[96] Jung, J. Y. et al. (2015). Wavelength-selective infrared metasurface absorber for multispectral thermal detection. *IEEE Photonics Journal*, 7(6): 1-10.